

# Balancing global water availability and use at basin scale in an integrated assessment model

Son H. Kim<sup>1</sup> · Mohamad Hejazi<sup>1</sup> · Lu Liu<sup>1</sup> · Katherine Calvin<sup>1</sup> · Leon Clarke<sup>1</sup> · Jae Edmonds<sup>1</sup> · Page Kyle<sup>1</sup> · Pralit Patel<sup>1</sup> · Marshall Wise<sup>1</sup> · Evan Davies<sup>2</sup>

Received: 9 April 2015 / Accepted: 6 January 2016 / Published online: 22 January 2016  
© Springer Science+Business Media Dordrecht (outside the USA) 2016

**Abstract** Water is essential for the world’s food supply, for energy production, including bioenergy and hydroelectric power, and for power system cooling. Water is already scarce in many regions of the world and could present a critical constraint as society attempts simultaneously to mitigate climate forcing and adapt to climate change, and to provide for a larger and more prosperous human population. Numerous studies have pointed to growing pressures on the world’s scarce fresh water resources from population and economic growth, and climate change. This study goes further. We use the Global Change Assessment Model to analyze interactions between population, economic growth, energy, land, and water resources simultaneously in a dynamically evolving system where competing claims on water resources from all claimants—energy, land, and economy—are reconciled with water resource availability—from renewable water, non-renewable groundwater and desalinated water sources—across 14 geopolitical regions, 151 agriculture-ecological zones, and 235 major river basins. We find that previous estimates of global water withdrawal projections are overestimated. Model simulations show that it is more economical in some basins to alter agricultural and energy activities rather than utilize non-renewable groundwater or desalinated water. This study highlights the importance of accounting for water as a binding factor in agriculture, energy and land use decisions in integrated assessment models and implications for global responses to water scarcity, particularly in the trade of agricultural commodities and land-use decisions.

---

**Electronic supplementary material** The online version of this article (doi:10.1007/s10584-016-1604-6) contains supplementary material, which is available to authorized users.

---

✉ Son H. Kim  
skim@pnnl.gov

<sup>1</sup> Joint Global Research Institute, Pacific Northwest National Laboratory, 5825 University Research Court, Suite 3500, College Park, MD 20740, USA

<sup>2</sup> University of Alberta, Edmonton, AB T6G 1H9, Canada

## 1 Introduction

Integrated assessment models (IAMs) have been used over the past several decades to understand the relationships between human and natural Earth systems in the context of climate change, and their use has contributed significantly to the assessment reports of the Intergovernmental Panel on Climate Change (IPCC). Integrated assessment modeling began in the 1970s with a focus on issues such as resource depletion, population growth, environmental pollution, and energy policy (Goodess et al. 2003). The 1990s witnessed the expansion in scope of several IAMs to include representations of climate, land-use, agriculture, and renewable energy. More recently, the IAM community has moved towards higher spatial resolution (regionalization), explicit accounting of climate change impacts, and incorporation of water within the IAM framework (e.g., Davies et al. 2013; Strzepek et al. 2013; Stehfest, et al. 2014). In the Fifth IPCC assessment, a suite of high resolution global IAMs has been used to generate the representative concentration pathways (RCPs) which are used by the climate modeling community to produce the fifth Coupled Model Intercomparison Project (CMIP5) (van Vuuren et al. 2012). Although IAMs carry detailed technological representations of the economy, energy, agriculture, land use, and climate systems, none of the IAMs used to generate the four RCPs incorporate the feedbacks between water supply and demand, and the rest of the systems modeled. That is, all assessments to date have implicitly derived emission pathways without explicitly considering the consequences of water limitations, or the interactions between hydrologic systems and human systems, as society adapts to and mitigates climate change. Yet, limits to hydrologic systems could impose constraints on both energy and land decisions, with significant effects on their resulting emissions. For example, global emission mitigation policies can significantly alter land use patterns (Wise et al. 2009), both by limiting land use change emissions, and by increasing bioenergy production; further, the future of bioenergy crops, an important component to many technology strategies to reduce greenhouse gas emissions, may depend critically on water availability (Berndes 2002). Hence, the ability to assess the implications of changing supplies and demands for water that stem from simultaneously-evolving human populations, economic systems, technologies, and climate, remains an important scientific goal.

Numerous studies have assessed various measures of water scarcity at alternative spatial scales (Vörösmarty et al. 2000; Wada et al. 2011; Hanasaki et al. 2013a; Hejazi et al. 2014a, b). These studies generally use information related to economic, food and energy demands—often derived from IAM simulations—as inputs to macro-scale global hydrologic and water management models, which are then used to assess the implications of growing demands for food and energy on water resources (Blanc et al. 2014; Hanasaki et al. 2013a; Voisin et al. 2013a). Many IAM teams have added water to their modeling suites, e.g., AIM: Hanasaki et al. 2013a,b; IGSM: Strzepek et al. 2013; Blanc et al. 2014; IMAGE: Gerten et al. 2013; Stehfest et al. 2014; MESSAGE: Damerau et al. 2015; ReMIND: Popp et al. 2011; Bonsch et al. 2014. These studies employ one-way coupling in which information is passed from IAMs to downstream models with no feedback to the economic decisions in IAMs. This assumes that even if the water supply in a particular basin is limited, alternative non-renewable water sources (e.g., unlimited fossil groundwater) or desalinated water are available without physical constraints or increasing costs; the approach also omits feedbacks with energy and land use decisions that would drive adoption of more water-efficient technologies and practices. In reality, extractable non-renewable groundwater supplies are limited, sometimes not exploitable

with current technologies, or are simply uneconomical. Moreover, both water demand and scarcity projections are critically dependent on the technologies assumed in the study (e.g., the evolution of irrigation efficiency and cooling technologies for thermoelectric cooling), which are often based on historical trends or preset assumptions within a model—factors that have contributed to the wide range of uncertainty in the estimates of future water scarcity. However, economic and technological responses to water scarcity are expected both in increasing water supplies, improving delivery efficiencies and reducing water demands that could alter long-term projections of water use.

This paper describes a novel approach to endogenizing water allocation decisions within an IAM framework, which couples energy, land use and water in code, simultaneously determining energy, land uses and derived water requirements, as well as reconciling feedbacks from binding water availability constraints on energy, agricultural production and land use, and other end-uses. Also explored are implications of water constraints on crop prices and the cost of water use, sectoral and regional impacts, and shifts in global agricultural trade. Additionally, a range of renewable water and non-renewable groundwater scenarios were generated to evaluate the sensitivity of modeling results to alternative assumptions of water availability. As an initial approach to balancing water demand and supply, we have chosen the river basin and annual time-step as the appropriate common scale that allows for estimates of water supply and demand where the economic decision integrates information on all agricultural goods and energy services, including water availability. Our initial effort is focused on understanding the major long-term regional and global drivers that lead to gross imbalances in the supply and demand for water resources.

## 2 Methodology

### 2.1 The Global Change Assessment Model (GCAM)

GCAM is a dynamic-recursive model combining representations of the global economy, the energy system, agriculture, land use, and climate (see Figure S1). The climate sub-model includes terrestrial and ocean carbon cycles, and a suite of coupled gas-cycle, climate, and ice-melt models (Calvin, et al. 2015). GCAM establishes market-clearing prices for all energy, agricultural and land markets in each 5-year time step from 2005 to 2100, such that supplies and demands for all markets are in equilibrium. This paper extends the recent addition of water supplies and demands to GCAM to ensure the conservation of water mass in the system by allocating water among competing users on an economic basis, subject to water availability at the basin scale. Components of water demand and supply have been developed in sequence over the past several years as documented below and combined in this paper for a comprehensive representation of the global water system.

GCAM currently tracks annual water demands for agricultural, energy, industrial, and municipal sectors at multiple spatial scales (see Figure S2) (Hejazi et al. 2014a, b). Agricultural water demand calculations are detailed, with derivations for twelve crop commodity classes at sub-regional scales (Chaturvedi et al. 2013). Industrial water demands are calculated for a wide range of technologies in GCAM's energy production and transformation sectors (Davies et al. 2013; Kyle et al. 2013), with the remainder of industrial water use assigned to manufacturing, which is modeled in an aggregate representation. Municipal estimates of water use are determined at a regional scale as a function of GDP per capita, water price, and a

technological-change parameter (Hejazi et al. 2013). The industrial and municipal sectors are represented in fourteen geopolitical regions, with the agricultural sector further disaggregated into as many as eighteen agro-ecological zones (AEZs) within each region. Base-year water demands—both withdrawals and consumptive use—are established by bottom-up estimates of water demand intensities of specific technologies and practices that are consistent with top-down regional and sectoral estimates of water use. The present study also accounts for in-stream water demands for uses such as ecosystem services, navigation, and recreation. This term is called the environmental flow requirement (EFR) and is estimated as 10 % of the long-term mean monthly natural streamflow following the work of Voisin et al. (2013b).

GCAM currently uses a global hydrologic module for the water supply that is based on a gridded monthly water balance model with a resolution of  $0.5^\circ \times 0.5^\circ$ . The GCAM hydrology module (see Hejazi et al. 2014a, b) requires gridded monthly precipitation, temperature, and maximum soil water storage capacity (a function of land cover) values, which are used to compute monthly evapotranspiration and runoff, and the soil moisture retention in the soil column. The water supply module has been evaluated against observational data and results of other models, and is used here to provide projections of water supply estimates to the end of the 21st century. For a more accurate representation of water supplies available for human use, GCAM has been updated to include a spatial river routing component – a modified representation of the River Transport Model (RTM) that employs a cell-to-cell routing scheme with a linear advection formula to simulate monthly natural streamflow.

## 2.2 Accessible water

The GCAM hydrology module provides estimates of renewable water resources for each of its river basins, which represent the maximum naturally-available annual water volumes in each basin. Some of this runoff flows too quickly to saline water bodies for capture, or occurs in remote areas where there is no potential human use. Thus, almost all recent studies have assessed water scarcity conditions using water scarcity indices such as that of Raskin et al. (1997), which compares total water demand to the total available amount of renewable water, and defines water-scarce regions as those in which total water demand is greater than 40 % of total water availability. In this paper, we follow the work of Postel et al. (1996) who estimated the proportion of total runoff that is potentially stable and accessible to humans as 1) the volume of impoundments behind dams, and 2) the volume of water in the form of baseflows (Postel et al. 1996). Thus, in this study, we define the volume of renewable water resources accessible for human use as:

$$QA_i^t = \max \left( 0, \min \left( QT_i^t - EFR_i, QB_i^t - EFR_i + RS_i \right) \right) \quad (1)$$

where  $QA_i^t$ ,  $QT_i^t$ , and  $QB_i^t$  are the annual volumes of accessible renewable water, natural streamflow and baseflow, respectively, in basin  $i$  and year  $t$ ;  $EFR_i$  is the environmental flow requirement for each basin, and  $RS_i$  is total reservoir storage capacity in each basin  $i$  in year 2005. The minimum function ensures that the combined baseflow and reservoir storage do not exceed total streamflow. All volumes are measured in  $\text{km}^3 \text{ years}^{-1}$ . According to the GRanD database (Lehner et al. 2011), the total reservoir storage volume globally is approximately  $6100 \text{ km}^3 \text{ years}^{-1}$ ; their geographic locations are then used to compute the total reservoir storage capacity in each basin – a quantity that is assumed constant over time in this analysis. As explained above,  $EFR_i$  is a function of the monthly average streamflow for each basin. Baseflow is computed as a fraction of annual streamflow following the estimates of Beck et al. (2013).

## 2.3 Non-renewable sources of water

In regions where the total water demands exceed the total accessible flow of renewable surface and ground water, non-renewable groundwater and desalinated water are also available for use. However, long-term use of non-renewable groundwater is unsustainable and desalination of brackish and saline water is expensive. The total water availability in each basin, including renewable water, non-renewable groundwater, and saline water, is estimated for calibration purposes to match current usage shares in the base year along with the associated cost of moving or treating water for human consumption.

Globally, Konikow (2011) estimated that global groundwater depletion from 1900 to 2008 totaled 4500 km<sup>3</sup>. Recent annual abstraction rates are in the range of 750–800 km<sup>3</sup> years<sup>-1</sup> (Shah et al. 2000), 728 km<sup>3</sup> years<sup>-1</sup> (Rost et al. 2008) and 734 km<sup>3</sup> years<sup>-1</sup> (Wada et al. 2010). Excessive groundwater depletion affects major regions of North Africa, the Middle East, South and Central Asia, North China, North America, and Australia, and localized areas throughout the world (Konikow and Kendy 2005). Wada et al. (2010) estimates non-renewable groundwater depletion at 309 km<sup>3</sup> years<sup>-1</sup> or 42 % of all groundwater withdrawals, while others give a range of non-renewable withdrawals at 400–800 km<sup>3</sup> years<sup>-1</sup>. Groundwater depletion has been increasing historically and the use of groundwater for irrigation has become impossible or cost-prohibitive in some of the most depleted areas (Dennehy et al. 2002).

To estimate groundwater pumping costs, we construct depletable resource supply curves for non-renewable groundwater (Table S1, Figure S3) using the following functional form (Deffeyes and MacGregor 1980):

$$\frac{Q}{Q_o} = \left( \frac{P}{P_o} \right)^\alpha \quad (2)$$

where  $Q$  is the volume of extracted groundwater at price  $P$ ;  $Q_o$  and  $P_o$  are initial groundwater extraction and current price estimates; and  $\alpha$  is the slope of the lognormal distribution. It is worth noting that the supply curve is continuous and rising in relation to the extraction cost of groundwater and simulates the increasing marginal cost of extracting the next unit of groundwater. This increasing rate of the cost is often associated with extracting more expensive resources (e.g., deeper, lower quality, more challenging environmental conditions, etc.). The use of this supply curve treats groundwater as a depletable resource and no groundwater recharge is assumed. The price and quantity of non-renewable groundwater demand is determined endogenously in GCAM based on the regional and global demand for freshwater.

Region-specific parameters are used for  $Q_o$ ,  $P_o$ , and a value of 0.5 for  $\alpha$  is assumed for all regions in the Baseline scenario, but a range of values are investigated to understand the relationship between groundwater availability and extraction cost and its impact on water demands. A value of 0.5 implies a nonlinear relationship, but that more groundwater is available at higher extraction cost.  $Q_o$  is estimated by back-calculating the amount of water that must be extracted from non-renewable groundwater sources to complement all the other available water resources in the year 2005 for each region.  $P_o$  is assumed to be a function of the energy cost associated with pumping groundwater from average water table depth following the work of Wang et al. (2012) and using Eq. 3:

$$P_o = \frac{d \cdot e \cdot g \cdot \rho}{3.6 \cdot 10^6 \cdot \eta} = \frac{d \cdot 0.2 \cdot 9.8 \cdot 1000}{3.6 \cdot 10^6 \cdot 0.5} = 0.0010889 \cdot d \quad (3)$$

Where  $d$  is the depth to groundwater (m),  $e$  is the energy cost rate (\$/kwh),  $g$  is the gravitational acceleration ( $\text{m/s}^2$ ),  $\rho$  is the density of water ( $\text{kg/m}^3$ ), and  $\eta$  is the pumping efficiency (dimensionless). Following the work of Wang et al. (2012), we use  $e=0.2$  \$/kWh,  $g=9.8$   $\text{m/s}^2$ ,  $\rho=1000$   $\text{kg/m}^3$ , and  $\eta=0.5$ . The median groundwater depth for each region is taken from the global water depth map of Fan et al. (2013). With the choice of  $\alpha$ , along with estimated values for  $Q_o$  and  $P_o$ , we establish non-renewable groundwater supply curves as a function of extraction cost for each of the GCAM region following Eq. 2.

In the year 2000, the global estimate of desalinated water was approximately  $4.6 \text{ km}^3 \text{ years}^{-1}$  – a critical resource in areas where there is insufficient renewable supply, such as the Middle East. Using FAO estimates of desalinated water at the country scale, we first downscale desalination values to a grid scale of  $0.5^\circ \times 0.5^\circ$  using the WWDR-II population data (Tobler et al. 1995) and coastal grids following the work of Wada et al. (2011), and then upscale to the basin scale for the year 2005 (see Figure S4). For expansion of desalination, we assume that the supply of saline water is infinite and that desalinated water is available for use where it is economically feasible. The cost of desalination is taken from the literature (Zhou and Tol 2005; Wangnick 2005) and summarized in Table S2. Although the industrial representation of our model accounts for all historical energy use, the projected energy requirements for desalination are not explicitly tracked at this time.

## 2.4 Balancing water supply and demand

Since water supplies and demands are estimated at multiple spatial and temporal resolutions, GCAM uses an internal mapping structure to ensure that water supplies and demands are in equilibrium at the basin scale. Specifically, GCAM allocates water among competing water users and solves for an inferred value of water (i.e., the shadow price of water) in each of the 235 global basins for each annual time period (see Figure S5). The equilibrium solution for water is simultaneously solved with all other goods and services in GCAM (e.g., energy, agriculture, land) to ensure internal consistency for any given time period. The three sources of water at the basin scale – accessible renewable water, non-renewable groundwater, and desalinated water – are nested within a logit structure and compete for the share of water supply; desalinated water is assumed to be available for non-irrigation purposes only. The logit formula is shown in Eq. 4 (Clarke and Edmonds 1993; Wise et al. 2014).

$$S_i = \frac{(\gamma_i \Pi_i)^\varphi}{\sum_{j=1}^3 (\gamma_j \Pi_j)^\varphi} \quad (4)$$

where  $\Pi_i$  is the median cost of option  $i$ ,  $\gamma_i$  is a scalar parameter, and  $\varphi$  is the logit exponent. Commonly used to describe consumer choice, the logit approach is used here to determine the share of water from each source to meet water demands in each basin. Accessible renewable water is assumed to be freely available, and is utilized prior to more expensive options of non-renewable groundwater or desalination. A nominal value for the cost of accessible renewable water is included to enable proper behavior of the logit formulation, however. When accessible renewable water supply is insufficient to meet total water demands in any given basin, the water price in that basin rises until higher cost

options provide additional supplies. Both nonrenewable groundwater and desalinated water may simultaneously contribute to supply in addition to the accessible renewable water. Changes in the water price propagates throughout the system and leads to changes in the costs of all goods and services that require water inputs, particularly agricultural goods, with corresponding readjustment of their demands. Given the large differential in water cost between the agricultural sectors and other end-uses such as electricity (see Table S3), we assume a subsidy that lowers the price of irrigated water by a factor of one hundredth – a value consistent with the study of Sağlam (2013), who reports that the agricultural sector pays substantially less than industry and households with a ratio around 1 %; i.e., agriculture pays only 1 % of the water price experienced by other sectors in a given river basin. If such a subsidy is ignored, GCAM cannot reproduce the estimated crop productions in the base year calibration as crop production is unprofitable with the associated water costs. Inclusion of subsidies and/or allocation rights for any particular sector is a capability within GCAM.

## 2.5 Uncertainty analysis

Since uncertainties in the estimations of several parameters and variables may affect our simulation results, we have extended the analysis to explore the range of uncertainty associated with the availability of accessible water and non-renewable groundwater. The range of accessible water values can be attributed to structural uncertainties associated with the hydrology model, the climate forcing and choice of general circulation model (GCM), and the baseflow calculation method for estimating the baseflow index parameters at the basin level. More specifically, the ensemble mean runoff and streamflow information are from a GCAM hydrology simulation under the SRES A2 emission scenario (no mitigation policy) as described in Hejazi et al. (2014b). Since the choice of hydrologic model implies a set of model biases, we also apply correction factors at the basin level to force the hydrology model to match the annual estimates of runoff in year 2005 to two reanalysis datasets: 1) the runoff data derived by the University of New Hampshire (UNH) by combining observed river discharge information from GRDC with a climate-driven water balance model (WBMc) (Fekete et al. 2000); 2) the runoff data derived from streamflow gauge data (Beck et al. 2013). Four GCMs (CGCM2, CSIRO2, HADCM3, PCM), as shown in Table 1, are used to force the hydrology model using the CRU climate dataset (Mitchell et al. 2004). The baseflow calculations are based on four methods as described by Beck et al. (2013).

Groundwater availability is affected by several factors, such as recharge rates, water table depths, and aquifer characteristics. Since the supply curve representation of groundwater in this study does not fully capture groundwater dynamics, sensitivity scenarios of the potential for groundwater availability is explored by assuming alternative groundwater depths and shape of the supply curve. We use 90th- and 10th-percentile estimated groundwater depths at the basin level instead of the median used previously (Figure S3, Table S1). Additionally, we assumed a wide range of values (0.2, 0.3, 0.4, 0.5, and 1) for  $\alpha$ , the slope of groundwater supply curve. A value of 1 implies a linear relationship, i.e., the cost of groundwater extraction and distribution increases linearly with depth. A lower value of  $\alpha$  results in a more rapidly increasing cost of groundwater extraction for each additional volume of groundwater depleted. Table 1 documents the full list of all the scenarios along with altered variables and their values.

**Table 1** List of all simulated scenarios for exploring the range of uncertainty associated with the estimates of accessible renewable water availability and the cost of non-renewable groundwater pumping and distributions

Altered variable	Method/Value	Scenario Name	Reference
Runoff	GCAM Hydrology	Baseline	Hejazi et al. 2014b
	Reanalysis data I (WBMc)	ScenAW1	Fekete et al. 2000
	Reanalysis data II (GSCD)	ScenAW2	Beck et al. 2013
Climate model (GCM)	Ens. mean	Baseline	Mitchell et al. 2004
	CGCM2	ScenAW3	Mitchell et al. 2004
	CSIRO2	ScenAW4	Mitchell et al. 2004
	HADCM3	ScenAW5	Mitchell et al. 2004
	PCM	ScenAW6	Mitchell et al. 2004
	Baseflow	Ens. mean	Baseline
Method 1 (BFI1)		ScenAW7	Beck et al. 2013 & ref. therein
Method 2 (BFI2)		ScenAW8	Beck et al. 2013 & ref. therein
Method 3 (BFI3)		ScenAW9	Beck et al. 2013 & ref. therein
Method 4 (BFI4)		ScenAW10	Beck et al. 2013 & ref. therein
Groundwater depth	Median	Baseline	Fan et al. 2013
	90 %	ScenGW1	Fan et al. 2013
	10 %	ScenGW2	Fan et al. 2013
Shape parameter $\alpha$	0.5	Baseline	This study
	1.00 (linear)	ScenGW3	This study
	0.40	ScenGW4	This study
	0.30	ScenGW5	This study
	0.20	ScenGW6	This study

### 3 Results

#### 3.1 Global water withdrawal projections

Global water withdrawal projections that do not consider supply limitations overestimate water use. In Fig. 1a, Baseline projections of global water withdrawals without supply limitations rise considerably by the middle of the century and remain above 6000 km<sup>3</sup> years<sup>-1</sup> throughout the century. In contrast, in the Baseline scenario with supply constraints, withdrawal volumes peak at 5500 km<sup>3</sup> years<sup>-1</sup> by the middle of the century and fall to 5000 km<sup>3</sup> years<sup>-1</sup> by 2100. Increasing demands for water and the rising cost of water withdrawals result in a peak-and-decline in global water withdrawals. Importantly, the uncertainty in accessible renewable water estimates (blue shading in Fig. 1a) is small relative to non-renewable groundwater estimates (red shading in Fig. 1a), indicating that the cost and availability of groundwater play a crucial role in determining the total global use of water.

Irrigation comprises the largest share of global water use and is also the most affected by constraining water use in the Baseline scenario as shown in Fig. 1b. Global withdrawals for irrigation decline significantly over time to a total reduction of approximately 20 % by 2100 relative to the irrigation withdrawals of the unconstrained scenario for the same year. Irrigation withdrawal volumes peak at 3900 km<sup>3</sup> years<sup>-1</sup> in 2050 and fall to 2900 km<sup>3</sup> years<sup>-1</sup> by 2100 in



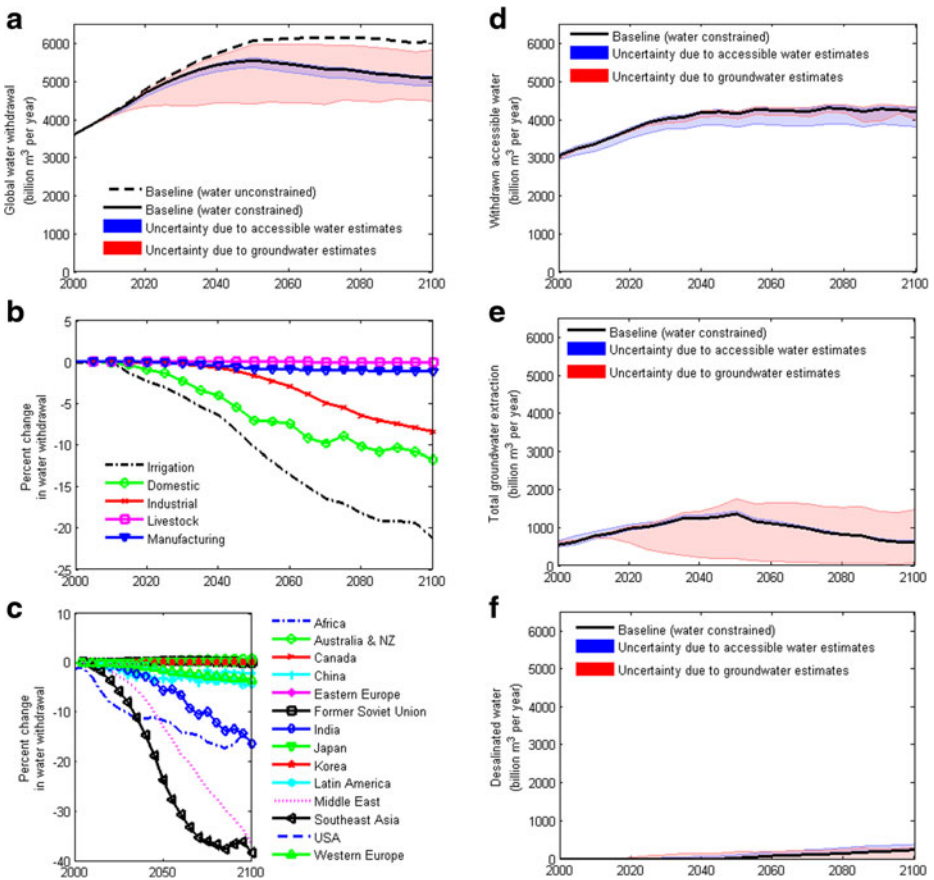


**Fig. 1** Global estimates of water withdrawals under the water constrained and unconstrained Baseline scenarios (a); the blue and red shaded areas represent the uncertainty associated with the calculations of accessible renewable water and non-renewable groundwater respectively; percent changes in water withdrawal when water is constrained in GCAM by sector (b) and by region (c); estimates of global water withdrawals from accessible renewable water (d), non-renewable groundwater (e), and desalinated water (f) sources

the constrained scenario. Irrigation withdrawal volumes capture withdrawal from all irrigated agriculture including biomass cultivation for energy purposes. Municipal and industrial (including energy) sector withdrawals are reduced by a smaller amount, with each sector contributing to about a 10 % reduction in 2100 relative to the unconstrained scenario. The sensitivity to the cost of water is greater for agriculture than for other uses since the relative cost of water for agricultural goods is a greater share of their total production cost (see Table S3 as an example).

Regionally, constraining water use affects those regions and basins where water is currently scarce. The Middle East, Africa, India and other Southeast Asia, with multiple basins at high water scarcity, are the most affected in the Baseline scenario. As indicated in Fig. 1c, withdrawals for Southeast Asia and the Middle East are reduced by approximately 40 %, and Africa and India by approximately 15 %, relative to the unconstrained scenario by 2100.

The global water withdrawal volume contributions by accessible renewable water, non-renewable groundwater and desalinated water sources are projected in Fig. 1d, e and f. Of the

three, accessible renewable water provides the largest contribution, and increases from approximately  $3000 \text{ km}^3 \text{ years}^{-1}$  in 2005 to greater than  $4000 \text{ km}^3 \text{ years}^{-1}$  by 2100 in the Baseline water constrained scenario. Non-renewable groundwater provides an important supplement to the limited renewable water supply, doubling from current withdrawals of approximately  $600 \text{ km}^3 \text{ years}^{-1}$  in 2005 to over  $1300 \text{ km}^3 \text{ years}^{-1}$  by 2050, before falling back to approximately  $600 \text{ km}^3 \text{ years}^{-1}$  by 2100. Rising costs of groundwater extraction, as shallow sources of water are depleted, drive this decline. Finally, while the relative contribution of desalinated water is small, the volume of desalinated water grows by more than an order of magnitude and reaches approximately  $250 \text{ km}^3 \text{ years}^{-1}$  by 2100 in the Baseline scenario.

Sensitivity scenarios for a range of alternative accessible renewable water and non-renewable groundwater assumptions indicate that uncertainties in non-renewable groundwater supplies have the greatest influence on total global water withdrawals over time – see Fig. 1e. Specifically, the range in non-renewable groundwater supply scenarios – from most pessimistic to most optimistic – shows between  $60$  and  $1500 \text{ km}^3 \text{ years}^{-1}$  of non-renewable annual groundwater contribution by 2100. Whereas, the maximum difference in the range of alternative accessible renewable water supplies is approximately  $500 \text{ km}^3 \text{ years}^{-1}$  (Fig. 1d), which is a third of the uncertainty range of the non-renewable groundwater withdrawal as explored in this analysis. We note that alternative assumptions of non-renewable groundwater supply have little influence on the contribution of accessible renewable water (see the red shading in Fig. 1d) since less-expensive renewable water is used prior to more-expensive non-renewable groundwater or desalinated water.

### 3.2 Changing views of global water scarcity

Changes in regional and sectoral water demands corresponding to the balancing of water supplies and demands are better represented at the basin scale, as areas of local water scarcity are widely distributed and more clearly displayed. The map of basin scarcity indices, defined in this study as the ratio of annual water withdrawal to annual accessible water, shows the severity and geographical heterogeneity of these changes for the year 2100 in Fig. 2. Panels in Fig. 2 display alternative views of basin scarcity between unconstrained and constrained scenarios and from sensitivity scenarios of water availability. Constraining water can be expected to have a greater impact in those regions and basins with high water scarcity. For these basins, economic responses to higher water costs lead to reductions in water use and lower scarcity indices. Changes in water scarcity are highlighted by the reduction of red shaded basins from the unconstrained Baseline scenario (Fig. 2a), to the constrained Baseline scenario (Fig. 2b), and further to the highest cost groundwater scenario (Fig. 2d). Thus, unconstrained scenarios of water use that do not consider economic responses to water use are likely to overestimate projections of future water scarcity.

### 3.3 The impact of constraining global water availability

One of the most important results of integrating the full global water cycle is the ability to explore potential regional and global economic responses to alternative water scarcity scenarios. We focus on agricultural impacts, since irrigation accounts for the largest component of global withdrawals and is the most-affected by water system constraints. Specifically, accounting for the cost of water withdrawals for irrigation, as well as for all other uses, affects the

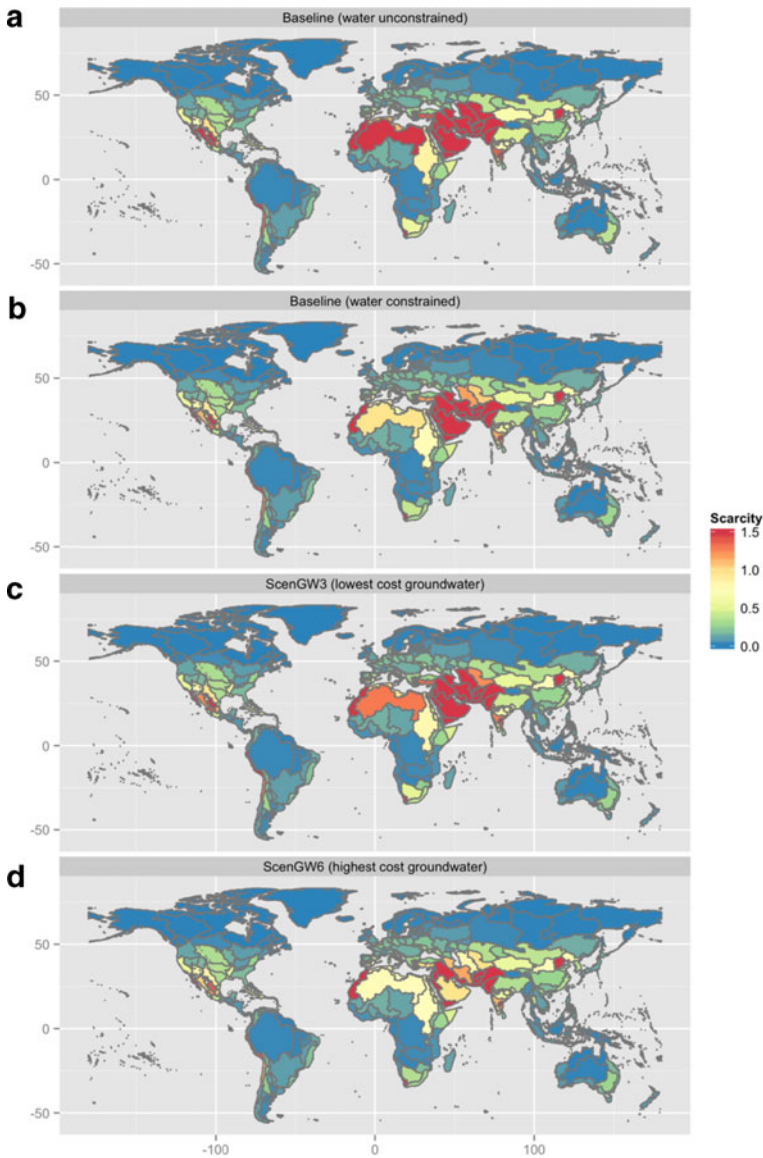


**Fig. 2** Estimates of water scarcity in year 2100 at the basin scale under the Baseline with unconstrained water (a), Baseline with constrained water (b), ScenGW3 with the lowest cost non-renewable groundwater (c), and ScenGW6 with the highest cost non-renewable groundwater (d) scenarios

production of crops by region. In addition, water costs have a differential impact on each crop type due to specific crop water requirements, crop prices and production costs, location of cropland, and the trade of agricultural goods.

The water impact on agricultural production at the AEZ scale is demonstrated in Fig. 3 for three of the most important grains, corn, rice and wheat, in the year 2100 for three alternative water supply scenarios, Baseline, ScenGW3, and ScenGW6. The non-renewable groundwater scenarios with the least (ScenGW3) and most (ScenGW6) expensive groundwater costs bound

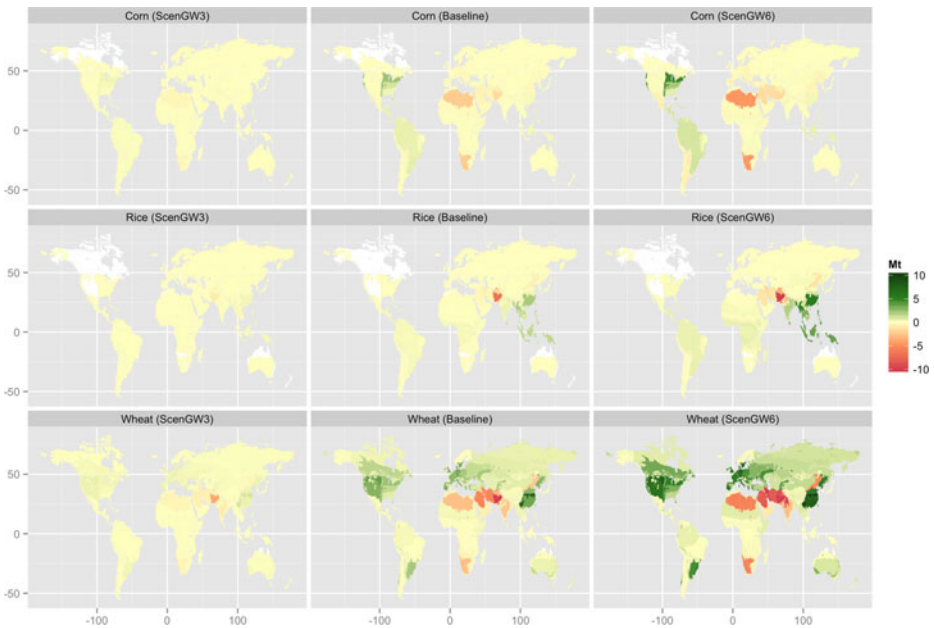


**Fig. 3** Changes in crop productions in million tons (Mt) for corn, rice, and wheat in 2100 between the water constrained and unconstrained cases for the Baseline (*middle panel*), lower bound ScenGW3 (*left panel*) and upper bound ScenGW6 (*right panel*) scenarios, respectively

the cost of water at the basin scale, and consequently the resulting impact to agricultural production. We note that assumptions regarding the cost and availability of groundwater are critical since non-renewable groundwater dictates water costs when withdrawals exceed the accessible renewable basin water supply. Figure 3 shows two primary impacts: the differential changes in the production of alternative crop types, and the regional responses of crop production to alternative water supply assumptions. Changes to wheat production are the most geographically dispersed, which is consistent with the widespread cultivation of wheat, while changes to corn and rice are more regionally limited (see also Figure S6). Reductions to production of each crop in water scarce regions are balanced through trade and the increased production of crops from those regions with more abundant and thus, lower-cost water. Changes to the regional production of all crops are increasingly more pronounced as the cost of water rises from scenario ScenGW3 to ScenGW6. We note that agricultural responses that result from the addition of water costs include assumed subsidies for irrigation water.

Increases in global agricultural trade mitigated regional impacts as the total global production of corn, rice and wheat fell by less than 1 % throughout the 21st century between the Baseline scenarios with and without water constraints (see Figure S7). Much larger changes in crop production occur at the local regional and AEZ scale, however. The corresponding global reduction in crop production raised the global commodity price of corn, rice and wheat by less than 5 %. In accounting for water availability and costs, assumptions that limit trade in agricultural goods and/or subsidies for irrigated water could result in greater reductions to global production and higher crop prices.

Other changes to the agricultural system are evident, such as the reduction in the share of irrigated relative to rain-fed crop production. However, options for more efficient irrigation technologies and improvements to the water distribution system that could provide a more

nuanced understanding of agriculture responses to water scarcity are not currently implemented.

Water scarcity and water pricing have a more moderate impact on the energy system. For instance, including the cost of water for electric power generation increases the competitiveness of natural gas combined-cycle plants with lower water requirements relative to thermal power plants. Efforts to include alternative cooling technology options and representation of energy production at a spatial resolution that is more consistent with the river-basin scale are underway to provide a more realistic and regional energy response to water availability. It is important to recognize, however, that multiple technology options exist for generating electricity and other energy forms with reduced water requirements that could limit the impact of water scarcity.

#### 4 Conclusions and future work

This paper introduces a new modeling capability within a fully-coupled energy-land-use-water system of an IAM for investigating the impact of regional water scarcity. This new capability includes the representation of water availability at the basin scale and three distinct sources of water, renewable surface and ground water, non-renewable groundwater and desalinated water. Long-term annual demands for water withdrawal from all end-uses are constrained by the availability of water at each basin. The constraint on water demands is achieved through a water pricing mechanism, in which the cost of water use propagates throughout the economy affecting regional agricultural production, energy technology choices and other demands for water.

Long-term projections of water use that do not account for water availability and constraints are likely to overestimate the use of water and scarcity in the long-term. The Baseline scenario in this analysis produced global water withdrawals nearly 20 % lower by the end of the century than a scenario without water-use constraints. Water scarce regions, such as the Middle East, Africa, India, and other Southeast Asia, and the agricultural sector with the largest water withdrawal were the most affected by the water constraints. There were several economic responses to the imposed water pricing at the basin scale, including changes in regional and global agriculture production, with reductions to agricultural outputs in water scarce regions. Reductions in agricultural production were offset through international trade and increased agricultural outputs from those regions with a more abundant water supply. While regional impacts for some basins were potentially large, international trade mitigated the net changes to global agriculture production.

Assumptions regarding non-renewable groundwater availability and extraction costs are key determinants of withdrawal projections, particularly in those regions with limited renewable surface water where groundwater is an important water source. Sensitivity cases exploring alternative non-renewable groundwater costs had a greater influence on the regional use of water than the sensitivity cases of accessible renewable water, which had a more limited range of water supply than non-renewable groundwater.

A basic representation of agricultural water subsidies was implemented to differentiate the cost of water across alternative end-users. These subsidies proved necessary to ensure consistency of the water costs with historical levels of regional agricultural production. Greater effort is necessary to understand the impact of regional water subsidies on sectoral responses within regions, as well as on the international trade of agricultural goods.

An internally consistent framework for investigating the responses to water availability and demand has been developed for additional analyses and future research. The fully coupled energy-land-use-water system enables the investigation of alternative climate mitigation and technology scenarios and their impact on water use. For instance, alternative levels of bioenergy production as a response to climate mitigation and their impact on the overall water system is now possible and currently under investigation. In addition, strategies to address demand responses to increasing water scarcity and higher water costs, such as improvements to irrigation technologies, distribution efficiencies, and other adaptive measures (e.g., re-use of wastewater) can be explored. Other ongoing activities include the explicit tracking of energy use in the water system, exploring the potential for interbasin transfers, and better characterization of groundwater recharge and aquifers.

Investigation of the appropriate temporal and spatial resolution for capturing water dynamics within the broader economic modeling framework of an integrated assessment model is an important aspect of our continuing research. Expansion of the GCAM water framework to subbasin and subannual hydrologic scale are under investigation for a more comprehensive understanding of the regional and global responses to water scarcity.

**Acknowledgments** This research was supported by the Office of Science of the U.S. Department of Energy through the Integrated Assessment Research Program. PNNL is operated for DOE by Battelle Memorial Institute under contract DE-AC05-76RL01830.

## References

- Beck HE, van Dijk AIJM, Miralles DG et al (2013) Global patterns in base flow index and recession based on streamflow observations from 3394 catchments. *Water Resour Res* 49(12):7843–7863
- Berndes G (2002) Bioenergy and water—the implications of large-scale bioenergy production for water use and supply. *Glob Environ Chang* 12(4):253–271
- Blanc E, Strzepek K, Schlosser A et al (2014) Modeling U.S. water resources under climate change. *Earth's Futur* 2(4):2013EF000214
- Bonsch M, Humpenöder F, Popp A et al (2014) Trade-offs between land and water requirements for large-scale bioenergy production. *GCB Bioenergy*. doi:10.1111/gcbb.12226
- Calvin K, Calrke L, Edmonds J et al (2015) GCAM Wiki Documentation. <https://wiki.umd.edu/gcam/>
- Chaturvedi V, Hejazi MI, Edmonds J et al (2013) Climate mitigation policy implications for global irrigation water demand. *Mitig Adapt Strateg Glob Chang*:1–19
- Clarke JF, Edmonds JA (1993) Modelling energy technologies in a competitive market. *Energy Econ* 15(2):123–129
- Damerau K, van Vliet O, Patt A (2015) Direct impacts of alternative energy scenarios on water demand in the Middle East and North Africa. *Clim Chang* 130(2):171–183
- Davies EGR, Kyle GP, Edmonds JA (2013) An integrated assessment of global and regional water demands for electricity generation to 2095. *Adv Water Resour* 52:296–313
- Deffeyes KS, MacGregor ID (1980) World uranium resources. *Sci Am* 242:66–76
- Dennehy KF, Litke DW, McMahon PB (2002) The high plains aquifer, USA: groundwater development and sustainability. *Geol Soc Lond, Spec Publ* 193(1):99–119
- Fan Y, Li H, Miguez-Macho G (2013) Global patterns of groundwater table depth. *Science* 339(6122):940–943
- Fekete BM, Vörösmarty CJ, Grabs W (2000) Global composite runoff fields based on observed river discharge and simulated water balances. Koblenz, Germany, Global Runoff Data Centre
- Gerten D, Lucht W, Ostberg S, et al (2013) Asynchronous exposure to global warming: freshwater resources and terrestrial ecosystems. *Environ Res Lett* 8(3), doi:10.1088/1748-9326/8/3/034032
- Goodess CM, Hanson C, Hulme M, Osborn TJ (2003) Representing climate and extreme weather events in integrated assessment models: a review of existing methods and options for development. *Integr Assess* 4(3):145–171
- Hanasaki N, Fujimori S, Yamamoto T et al (2013a) A global water scarcity assessment under shared socio-economic pathways; Part 2: water availability and scarcity. *Hydrol Earth Syst Sci* 17(7):2393–2413
- Hanasaki N, Fujimori S, Yamamoto T et al (2013b) A global water scarcity assessment under Shared Socio-economic Pathways – Part 1: water use. *Hydrol Earth Syst Sci* 17:2375–2391

- Hejazi MI, Edmonds J, Chaturvedi V et al (2013) Scenarios of global municipal water use demand projections over the 21st century. *Hydrol Sci J - J Sci Hydrol* 58(3):519–538
- Hejazi MI, Edmonds J, Clarke L et al (2014a) Long-term global water projections using six socioeconomic scenarios in an integrated assessment modeling framework. *Technol Forecast Soc Chang* 81:205–226
- Hejazi MI, Edmonds J, Clarke L et al (2014b) Integrated assessment of global water scarcity over the 21st century under multiple climate change mitigation policies. *Hydrol Earth Syst Sci* 18(8):2859–2883
- Konikow LF (2011) Contribution of global groundwater depletion since 1900 to sea-level rise. *Geophys Res Lett* 38(17), L17401
- Konikow LF, Kendy E (2005) Groundwater depletion: a global problem. *Hydrogeol J* 13(1):317–320
- Kyle GP, Davies EGR, Dooley JJ et al (2013) Influence of climate change mitigation technology on global demands of water for electricity generation. *Int J Greenh Gas Control* 13:112–123
- Lehner B, Liermann CR, Revenga C et al (2011) High-resolution mapping of the world's reservoirs and dams for sustainable river-flow management. *Front Ecol Environ*
- Mitchell TD, Carter TR, Jones PD et al (2004) A comprehensive set of high-resolution grids of monthly climate for Europe and the globe: the observed record (1901–2000) and 16 scenarios (2001–2100). Tyndall Centre Working Paper 55. Norwich, UK, Tyndall Centre for Climate Change Research, University of East Anglia
- Popp A, Dietrich J, Lotze-Campen H, Klein D et al (2011) The economic potential of bioenergy for climate change mitigation with special attention given to implications for the land system. *Environ Res Lett* 6, 034017. doi:10.1088/1748-9326/6/3/034017, <http://iopscience.iop.org/1748-9326/6/3/034017>
- Postel SL, Daily GC, Ehrlich PR (1996) Human appropriation of renewable fresh water. *Science* 271(5250):785–788
- Raskin P, Gleick P, Kirshen P et al (1997) Water futures: assessment of long-range patterns and prospects. Stockholm, Stockholm Environment Institute
- Rost S, Gerten D, Bondeau A et al (2008) Agricultural green and blue water consumption and its influence on the global water system. *Water Resour Res* 44(9), W09405
- Sağlam Y (2013) Pricing of water: optimal departures from the inverse elasticity rule. *Water Resour Res* 49(12): 7864–7873
- Shah T, Molden D, Sakthivadivel R, Seckler D (2000) The global groundwater situation: overview of opportunities and challenges. *Int Water Manag Inst*
- Stehfest E, D van Vuuren, T Kram et al (2014) Integrated Assessment of Global Environmental Change with IMAGE 3.0, Model description and policy applications, The Hague: PBL Netherlands Environmental Assessment Agency
- Strzepek K, Schlosser A, Gueneau A, Gao X, Blanc É, Fant C, Rasheed B, Jacoby HD (2013) Modeling water resource systems within the framework of the MIT Integrated Global System Model: IGSM-WRS. *J Adv Model Earth Syst* 5(3):638–653
- Tobler W, Deichmann U, Gottsegen J, Maloy K (1995) The global demography project. Santa Barbara CA, National Center for Geographic Information and Analysis
- van Vuuren DP, Riahi K, Moss R et al (2012) A proposal for a new scenario framework to support research and assessment in different climate research communities. *Glob Environ Chang* 22(1):21–35
- Voisin N, Liu L, Hejazi M et al (2013a) One-way coupling of an integrated assessment model and a water resources model: evaluation and implications of future changes over the US Midwest. *Hydrol Earth Syst Sci* 17(11):4555–4575
- Voisin N, Li H, Ward D et al (2013b) On an improved sub-regional water resources management representation for integration into earth system models. *Hydrol Earth Syst Sci* 17(9):3605–3622
- Vörösmarty C, Green P, Salisbury J, Lammers R (2000) Global water resources: vulnerability from climate change and population growth. *Science* 289(5477):284–288
- Wada Y, van Beek LPH, van Kempen CM et al (2010) Global depletion of groundwater resources. *Geophys Res Lett* 37(20), L20402
- Wada Y, van Beek L, Viviroli D et al (2011) Global monthly water stress: 2. Water demand and severity of water stress. *Water Resour Res* 47(7), W07518
- Wang J, Rothausen S, Conway D et al (2012) China's water-energy nexus: greenhouse-gas emissions from groundwater use for agriculture. *Environ Res Lett* 7(1):014035
- Wangnick/GWI (2005) Worldwide desalting plants inventory. Global Water Intelligence, Oxford
- Wise M, Calvin K, Thomson A et al (2009) Implications of limiting CO<sub>2</sub> concentrations for land use and energy. *Science* 324(5931):1183–1186
- Wise M, Calvin K, Kyle GP et al (2014) Economic and physical modeling of land use in GCAM 3.0 and an application to agricultural productivity, land, and terrestrial carbon. *Clim Chang Econ* 05(02):1450003
- Zhou Y, Tol RSJ (2005) Evaluating the costs of desalination and water transport. *Water Resour Res* 41(3), W03003